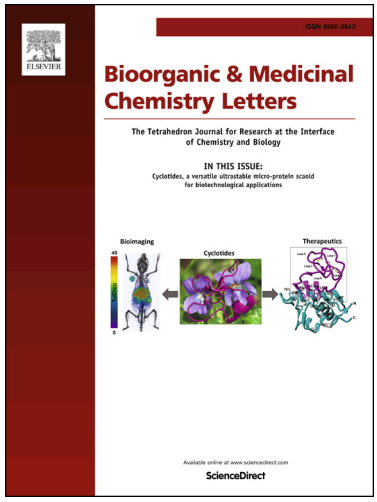

Discovery of 4-Ethoxy-7*H*-pyrrolo[2,3-*d*]pyrimidin-2-amines as Potent, Selective and Orally Bioavailable LRRK2 Inhibitors

Xiao Ding, Luigi Piero Stasi, Ming-Hsun Ho, Baowei Zhao, Hailong Wang, Kai Long, Qiongfeng Xu, Yingxia Sang, Changhui Sun, Huan Hu, Haihua Yu, Zehong Wan, Lizhen Wang, Colin Edge, Qian Liu, Yi Li, Kelly Dong, Xiaoming Guan, F. David Tattersall, Alastair D. Reith, Feng Ren

PII: S0960-894X(18)30238-5
DOI: https://doi.org/10.1016/j.bmcl.2018.03.045
Reference: BMCL 25699

To appear in: *Bioorganic & Medicinal Chemistry Letters*

Received Date: 2 January 2018
Revised Date: 17 March 2018
Accepted Date: 17 March 2018

Please cite this article as: Ding, X., Stasi, L.P., Ho, M-H., Zhao, B., Wang, H., Long, K., Xu, Q., Sang, Y., Sun, C., Hu, H., Yu, H., Wan, Z., Wang, L., Edge, C., Liu, Q., Li, Y., Dong, K., Guan, X., Tattersall, F.D., Reith, A.D., Ren, F., Discovery of 4-Ethoxy-7*H*-pyrrolo[2,3-*d*]pyrimidin-2-amines as Potent, Selective and Orally Bioavailable LRRK2 Inhibitors, *Bioorganic & Medicinal Chemistry Letters* (2018), doi: https://doi.org/10.1016/j.bmcl.2018.03.045

Graphical Abstract

To create your abstract, type over the instructions in the template box below.
Fonts or abstract dimensions should not be changed or altered.

Discovery of 4-Ethoxy-7*H*-pyrrolo[2,3-*d*]pyrimidin-2-amines as Potent, Selective and Orally Bioavailable LRRK2 Inhibitors

Leave this area blank for abstract info.

Xiao Ding[a], Luigi Piero Stasi[a], Ming-Hsun Ho[b], Baowei Zhao[a], Hailong Wang[a], Kai Long[a], Qiongfeng Xu[a], Yingxia Sang[a], Changhui Sun[a], Huan Hu[a], Haihua Yu[a], Zehong Wan[a], Lizhen Wang[a], Colin Edge[c], Qian Liu[b], Yi Li[b], Kelly Dong[b], Xiaoming Guan[a], F. David Tattersall[a], Alastair D. Reith[d], Feng Ren*[, a]

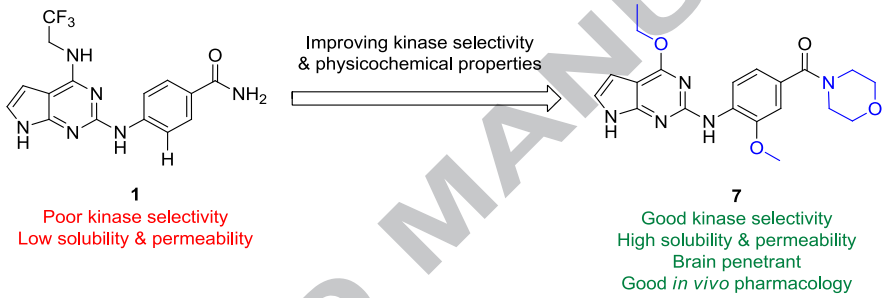

Bioorganic & Medicinal Chemistry Letters
journal homepage: www.elsevier.com

Discovery of 4-Ethoxy-7*H*-pyrrolo[2,3-*d*]pyrimidin-2-amines as Potent, Selective and Orally Bioavailable LRRK2 Inhibitors

Xiao Ding[a], Luigi Piero Stasi[a], Ming-Hsun Ho[b], Baowei Zhao[a], Hailong Wang[a], Kai Long[a], Qiongfeng Xu[a], Yingxia Sang[a], Changhui Sun[a], Huan Hu[a], Haihua Yu[a], Zehong Wan[a], Lizhen Wang[a], Colin Edge[c], Qian Liu[b], Yi Li[b], Kelly Dong[b], Xiaoming Guan[a], F. David Tattersall[a], Alastair D. Reith[d], Feng Ren*[, a]

[a]*Neurodegeneration DPU, Neurosciences Therapeutic Area Unit, GSK Pharmaceuticals R&D, 898 Halei Road, Zhangjiang Hi-Tech Park, Pudong, Shanghai 201203, PR China.*

[b]*Platform Technology Sciences, GSK Pharmaceuticals R&D, 898 Halei Road, Zhangjiang Hi-Tech Park, Pudong, Shanghai 201203, PR China.*

[c]*Platform Technology Sciences, GSK Pharmaceuticals R&D, Medicines Research Centre, Gunnels Wood Road, Stevenage, Herts UK.*

[d]*Neurodegeneration DPU, Neurosciences Therapeutic Area Unit, GSK Pharmaceuticals R&D, Medicines Research Centre, Gunnels Wood Road, Stevenage, Herts, UK.*

**Corresponding author. Tel.: +86 18616743377; fax: +86 021 61590730; e-mail address: 2648666968@qq.com (F. Ren).*

ARTICLE INFO

Article history:
Received
Revised
Accepted
Available online

Keywords:
pyrrolo[2,3-d]pyrimidine
LRRK2
Parkinson's disease
kinase selectivity
CNS penetration.

ABSTRACT

Inhibition of LRRK2 kinase activity with small molecules has emerged as a potential novel therapeutic treatment for Parkinson's disease. Herein we disclose the discovery of a 4-ethoxy-7H-pyrrolo[2,3-d]pyrimidin-2-amine series as potent LRRK2 inhibitors identified through a kinase-focused set screening. Optimization *of* the physicochemical properties and kinase selectivity led to the discovery of compound **7**, which exhibited potent in vitro inhibition of LRRK2 kinase activity, good physicochemical properties and kinase selectivity across the kinome. Moreover, compound **7** was able to penetrate into the CNS, and *in vivo* pharmacology studies revealed significant inhibition of Ser935 phosphorylation in the brain of both rats (30 and 100 mg/kg) and mice (45 mg/kg) following oral administration.

Parkinson's disease (PD) is a slow, progressive and second most common neurodegenerative disease which affects over 10 million people worldwide.[1,2] Numerous treatments have been developed including L-DOPA, dopamine agonists, MAO-B inhibitors,[1] but these compounds relieve the symptoms rather than the progression of the disease. The development of disease-modifying therapies therefore represents an unmet medical need.[3] Through genome-wide association studies (GWAS), a number of variants in genes such as those for α-synuclein, leucine-rich repeat kinase 2 (LRRK2), Parkin and PTEN induced putative kinase 1 (PINK1) have been reported to be associated with increased risk of developing PD.[4] Such variants in LRRK2 constitute the most common genetic cause of familial PD.[5] In particular, the most frequent G2019S mutation increases kinase activity, suggesting that restoringLRRK2 kinase activity to normal in the brain could be a potential therapeutic target for the treatment of PD.[6]

In the past several years a number of small molecule LRRK2 inhibitors with distinct chemical structures have been disclosed[7,8] including 2,4-diaminopyrimidine,[9] indazole,[10] pyrrolopyrimidine,[11] indolinone[12] and 3-cyanoquinoline[13] cores. Several representative compounds such as GNE-9605,[9] PF-06447475,[11] and MLi-2[10] exhibited reasonable pharmacokinetic (PK) profile with good central nervous system (CNS) penetration and reasonable kinase selectivity. Many of these compounds significantly reduced LRRK2 phosphorylation, (a surrogate measure of the inhibition of LRRK2 kinase) both *in vitro* and *in vivo*. Our group recently patented several novel scaffolds of LRRK2 kinase inhibitors with high potency and good kinase selectivity, including 5-substituent-*N*-arylbenzamide[14] and 4-substituent-7*H*-pyrrolo[2,3-*d*]pyrimidin-2-amine series[15,16]. The benzamide compound we discovered, GSK2578215A, demonstrated potent LRRK2 kinase inhibition and high selectivity across the kinome[17-18]. This compound has been widely used as a tool molecule for the exploration of the biology of LRRK2[19,20]. Herein, we describe the discovery of the 4-substituted-7*H*-pyrrolo[2,3-*d*]pyrimidin-2-amine series as potent LRRK2 kinase inhibitors and the lead optimization focusing on improving the series' physicochemical properties and kinase

selectivity. Extensive structure-activity relationship (SAR) studies led to the discovery of a potent and selective LRRK2 inhibitor **7**, which significantly inhibited Ser935 phosphorylation in brain of both rats (30 and 100 mg/kg) and mice (45 mg/kg) following oral administration.

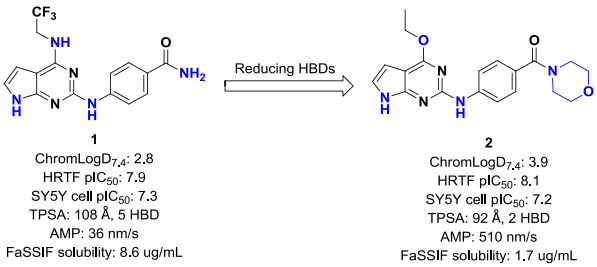

Scheme 1. Structures and profile of compounds **1** and **2**

Our work was initiated from a kinase-focused set screening (KCS) of GSK in house compounds by measuring the inhibition of LRRKtide phosphorylation using a homogeneous time-resolved fluorescence (HTRF) assay. Compound **1** (Scheme 1) was identified as a hit with good LRRK2 inhibitory potency in the HTRF assay (pIC_{50} = 7.9), and the activity was confirmed in a SH-SY5Y cell assay where the effect on the phosphorylation of LRRK2 Ser935 was measured. Compounds of similar chemotypes have been widely reported as inhibitors of kinases such as SYK[21] and JAK[22]. Compound **1** was then docked in the LRRK2 homology model,[18] and was suggested to reside in the ATP binding pocket of LRRK2 kinase (Figure 1). The scaffold 7*H*-pyrrolo[2,3-*d*]pyrimidin-2-amine formed three hydrogen-bond interactions with the backbone of Glu1948 and Ala1950 in the hinge region, and had close contact with the gatekeeper residue Met1947. The 2,2,2-trifluoroethyl chain located inside the pocket and pointed toward the residue His1998, while the amide group pointed toward the solvent-exposed area.

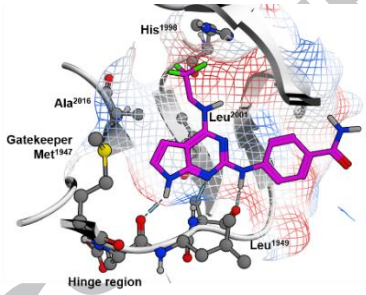

Figure 1. Predicted docking pose of compound **1** (purple) in the LRRK2 homology model (gray). Intermolecular hydrogen-bond interactions are shown as blue dashed lines.

Further profiling of compound **1** revealed poor artificial membrane permeability (AMP, 36 nm/s) and low solubility in fasted state simulated intestinal fluids (FaSSIF, 8.6 μg/mL). We attributed these poor physicochemical properties partly to its high topological polar surface area (TPSA, 109 Å) and the presence of five hydrogen-bond donors (HBDs) in the molecule. In addition, high PSA and more HBDs have been reported to be detrimental to CNS penetration properties (TPSA ≤ 90 Å and HBDs ≤ 2 were recommended for CNS compounds).[23] Initially, we focused on reducing the molecules' HBDs. Based on the modeling structure (Figure 1), the two hydrogens on the 7*H*-pyrrolo[2,3-*d*]pyrimidin-2-amine scaffold had to be maintained because they involved in the bindings with the LRRK2 hinge region which are pivotal for potency. Further investigation revealed that primary amide group pointed towards the solvent region could be replaced with other hydrophilic amides such as morpholinol amide. In addition, the 2,2,2-trifluoroethyl amine, which formed hydrophobic interaction with the LRRK2 protein, could be replaced with lipophilic alkoxyl groups. Compound **2** (Scheme 1) was thus quickly identified as a new hit with only two HBDs and good potency both in HTRF (pIC_{50} = 8.1) and cellular assays (pIC_{50} = 7.2). Not surprisingly, compound **2** showed much improved membrane permeability (AMP = 510 nm/s) with a reasonable TPSA of 92 Å. The FaSSIF solubility of compound **2** remained low (1.7 μg/mL) and required further optimization. Both compounds **1** and **2** were progressed to kinase selectivity assessment using standard radioactivity-based enzymatic assays against a panel of 140 kinases,[24] and at the concentration of 1 μM, they exhibited inhibitory activities of greater than 50% on 72 and 61 kinases, respectively, including inhibition of MAP4K3, MLK1, JAK2, IRAK4, and SYK. Thus, a significant improvement of the kinase selectivity profile was critical for further progression of the series.

Table 1. LRRK2 inhibition and kinase selectivity for compounds **2**–**13**

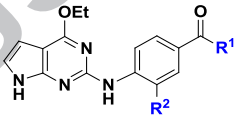

Cmpd	R^1	R^2	Cell pIC_{50}[a]	HTRF pIC_{50}	KS[b]
2		H	7.2	8.1	61/140
3	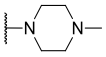	H	7.1	7.9	ND[c]
4	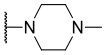	F	6.8	7.9	32/140
5	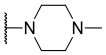	Cl	6.6	7.9	20/140
6	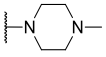	OCH_3	6.8	7.8	17/140
7		OCH_3	6.8	7.9	12/140
8	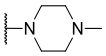	OCH_2CH_3	6.9	8.0	9/140
9		OCH_2CH_3	6.7	8.0	12/140
10	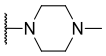	$OCH(CH_3)_2$	6.4	8.0	1/140
11		$OCH(CH_3)_2$	6.2	7.9	ND[c]
12	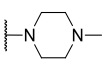	$OCHF_2$	6.8	>9.8	14/140
13	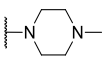	$N(CH_3)_2$	5.5	6.7	ND[c]

[a]The average of at least two determinations.
[b]Kinase selectivity (KS) was measured using standard radioactivity-based enzymatic assays against a panel of 140 kinases (Dundee profiling) at 1 μM: data are shown as numbers of kinases displaying >50% activity.
[c]Not determined.

Table 2. LRRK2 potency, developability, and kinase selectivity for compounds **7**, **14**–**22**

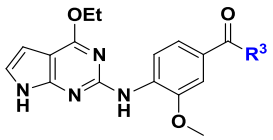

Cmpd	R^3	Cell pIC_{50}[a]	HTRF pIC_{50}	*h*Cli[b] (mL/min/g)	Pgp/BCRP[c] PR[d]/ PP(nm/s)[e]	Solubility[f] (μg/mL)	ClogD[g]	PFI[h]	KS[i]
7		6.8	7.9	1.1	3.1/319	127.3	4.5	7.5	12/140
14	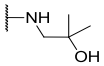	6.9	7.9	0.8	3.8/56	25.5	4.1	7.1	14/140
15		7	8.1	1.4	1.8/406	153.7	5.0	8.0	15/140
16		7.1	7.8	0.8	2.2/294	78.8	5.1	8.1	17/140
17		6.7	7.2	1.5	ND[j]	4.4	5.7	8.7	ND[j]
18		6.5	8.2	1.1	1.5/276	39.7	5.7	8.7	12/140
19		6.8	7.2	1.1	ND[j]	6.2	4.3	7.3	ND[j]
20		7.2	8.2	<0.777	5.0/84	620.7	3.0	6.3	ND[j]
21		7.1	8.5	3.2	2.3/294	309.4	4.9	7.9	ND[j]
22		6.8	8.1	2.5	4.0/270	300.1	4.9	7.9	17/140

[a]The average of at least two determinations. [b]*In vitro* human liver microsomal clearance. [c]MDCKII-MDR1 transduced with BacMam2-BCRP cell line. [d]Permeability ratio, A→B (apical to basolateral) with GF120918/A→B without GF120918. [e]Passive Permeability, A→B with GF120918. [f]FaSSIF Solubility was measured after 4 h incubation. [g]Measured $ChromLogD_{7.4}$. [h]PFI = Chrom log $D_{pH7.4}$ + # Ar. [i]Kinase selectivity, standard radioactivity-based enzymatic assays against a panel of 140 kinases (Dundee profiling) at 1 uM, quoted as numbers of kinase displaying >50% activity. [j]Not determined.

The poor kinase selectivity of compounds **1** and **2** was proposed to be due to the binding in the ATP pocket, which is highly conserved across the human kinome. Unique structure motifs or functional groups to enable more selective specific interaction(s) of compounds with LRRK2 kinase over other protein kinases might provide improved selectivity. Our homology model showed that among the 21 residues which formed the ATP binding pocket of LRRK2, five resided in close contact with the docked compound **1** and **2**, i.e. Met1947, Leu1949, His1998, Leu2001, and Ala2016 (Figure 1 and Figure S1). Multiple sequence alignments of these specific bind binding site residues were performed across the human kinome of LRRK2 over other kinases.[25,26] Among these, Leu1949 was identified as the most distinct residue for LRRK2 and 60% of its equivalent residue in other human kinases was determined to be either Tyr or Phe, which were larger in size than Leu. Leu1949 resided in close contact of the R^2 group of the series (Table 1), and we thus started to explore SAR on R^2 aiming for specific interaction(s) with LRRK2 over other kinases for improved kinase selectivity.

As illustrated in Table 1, compounds with various substituents on R^2 position were synthesized, and their potency and kinase selectivity were determined. Most of the compounds demonstrated comparable or slightly compromised LRRK2 inhibitory potency compared to compound **2,** and significant improvement of kinase selectivity was achieved. For instance, introducing halo groups such as fluoro (**4**) or chloro (**5**) on the R^2 position resulted in slightly decreased cellular potency and much improved kinase selectivity, hitting only 32 and 20 kinases out of the 140-kinase panel with over 50% inhibition at 1 μM concentration, respectively. Side-by-side comparisons among compounds **4–6** and **8** revealed that increasing the sizes at the R^2 position resulted in the improvement of kinase selectivity (OCH_2CH_3 > OCH_3 ≈ Cl > F). This observation was consistent with our homology model and the literature reports of similar structural scaffolds, that alkoxy groups with appropriate sizes were favored for the R^2 binding pocket of LRRK2 over other kinases.[27,28] Further increasing the steric hindrance of the R^2 substitution (**10**) led to significant reduction of LRRK2 potency especially in the cell-based assay, even though the kinase selectivity was excellent (only 1 out of 140 kinases was inhibited with > 50% at 1 μM of compound **10**). The homology model also suggested that the R^2 group was projected proximity to Leu1949 of the LRRK2 binding pocket and therefore steric bulky substituents such as isopropoxy (**10** and **11**) and dimethylamino (**13**) were not well tolerated. Considering the potential de-methylation metabolism risk of the *N*-methyl piperazine analogues, the morpholine derivatives (compounds **7**, **9**, and **11**) were favored. Among them, compound **7** was selected for further progression due to its lower molecular weight than compound **9** and higher potency than compound **11**. Further profiling of compound **7** revealed good metabolic stability in liver microsomes (Cli = 1.1 mL/min/g)[29] and good solubility in FaSSIF (127.3 μg/mL). Kinase selectivity of **7** was further evaluated using the HotSpot assay platform of over 340 other kinases and it was confirmed a highly selective LRRK2 inhibitor with only three kinases (ALK, IRR and TSSK1) exhibiting an ambit score of <10 in the KINOMEscan profile[30].

We then focused our SAR on the exploration of the amide group (R^3) aiming to further improve the overall developability profile (Table 2). Property forecast index (PFI),[31] determined from calculated or measured ChromlogD (pH = 7.4), was reported as a key indicator for compounds' developability properties, thus we designed our compounds with PFIs < 9. A variety of different amide groups with diversified steric and electronic properties was well tolerated with good potency in both cell and HTRF assays, including acyclic (**14**), cyclic (**15**–**18**), spiro- (**19** and **20**), and fused- (**21** and **22**) amides. The observation was consistent with the predicted binding mode that the amide group pointed towards the opened solvent-exposed area of LRRK2 kinase, enabling the tolerance of substitutions in this region. All the tested compounds demonstrated good metabolic stability in human liver microsomes with intrinsic clearance less than 3 mL/min/g except for compounds **21** (3.2 mL/min/g). None of them was a significant Pgp/BCRP efflux transporter substrate when measured in a MDCKII cell line double-transduced with human Pgp and BCRP transporters, in combination with the high passive permeability (> 100 nm/s except for compounds **14** and **20**), indicating the potential good CNS penetration property of these compounds. Relatively lower passive permeability (< 100 nm/s) was observed for compounds **14** and **20** which might be due to an additional HBD for **14** and higher basicity for **20**. Moreover, most of compounds showed good FaSSIF solubility (>100 μg/mL) except for compounds **14** and **16**–**19**. Several compounds were further screened in a panel of 140 kinases and they all showed comparable kinase selectivity as compound **7**.

Table 3. PK profile of compounds **7** and **22** in rats

Cmpd	$DNAUC_{0-t}$ in blood[c]	$DNAUC_{0-t}$ in brain	K_p (br/bl)	Fu% in brain[d]
7[a]	1034	252	0.24	1.0
22[b]	487	246	0.51	<0.5

[a]10 mg/kg, oral dosing. [b]2 mg/kg, oral dosing. [c]DNAUC = dose normalized area under the curve, (ng·h/mL(g))/(mg/kg). [d]Free fraction in rat brain.

With the balanced profile of potency, permeability, solubility, and metabolic stability, compounds **7** and **22** were progressed to *in vivo* evaluation for their CNS penetration and pharmacokinetic properties after dosing by oral gavage at 10 mg/kg and 2 mg/kg, respectively (compound **5** demonstrated very similar profile as **7** but with slightly less favored kinase selectivity, in combination with their high structure similarity, compound **5** was de-selected for further progression). As shown in Table 3, both compounds **7** and **22** exhibited good CNS exposure in rats with brain to blood ratios of 0.24 and 0.51, respectively, as measured by total drug concentrations. However, compound **22** was observed lower unbound fraction in rat brain (<0.5%) in comparison to **7** (1.0 %). Given the superior free unbound fraction, in combination with its good oral exposure especially in brain, compound **7** was progressed to an *in vivo* pharmacodynamic (PD) study.

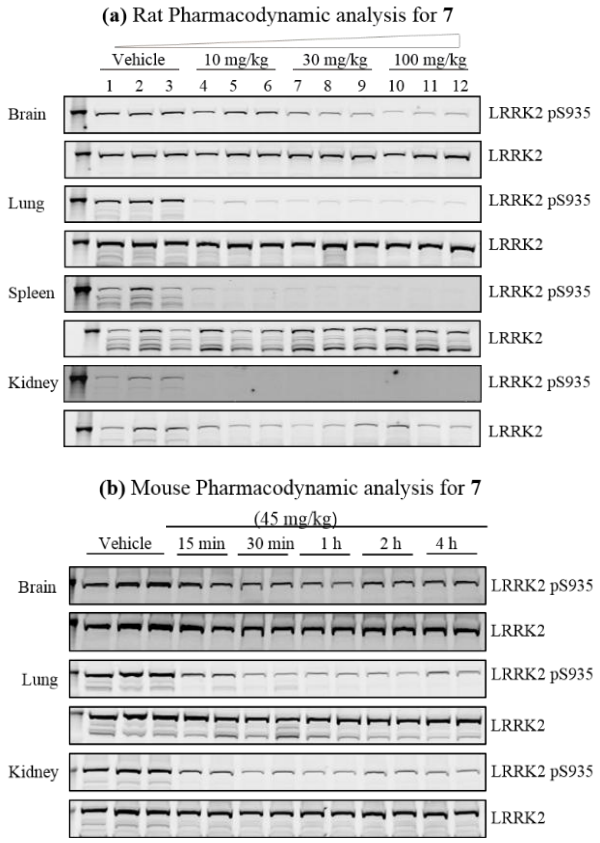

Figure 2. (a) Pharmacodynamic analysis for compound **7** in Han Wistar rats. (b) Pharmacodynamic analysis for compound **7** in C57/BL6 mice. Pharmacodynamic study of compound **7** from brain, spleen, lung and kidney following oral gavage at the indicated doses. Tissues were collected, and endogenous LRRK2 was resolved in SDS-PAGE followed by western blot with an antibody directed against LRRK2 phospho-Ser935 or total LRRK2.

Prior to the *in vivo* PD evaluation, we firstly confirmed the *in vitro* pharmacology of compound **7** on endogenous LRRK2 in human lymphoblastoid cells derived from a healthy subject (AHE) and a Parkinson's disease patient with homozygous LRRK2[G2019S] mutation (ANK)[32]. A concentration-dependent inhibition of LRRK2 Ser935 phosphorylation was observed with measured pIC_{50} values of 7.5 in AHE and 7.8 in ANK. The *in vivo* pharmacology of **7** was then evaluated by measuring inhibition of LRRK2 Ser935 phosphorylation in brain, lung, spleen, and kidney following oral administration to rats at 10 mg/kg, 30 mg/kg and 100 mg/kg (Figure 2a). Compound **7** demonstrated dose dependent reductions on phosphorylation of LRRK2 Ser935 in brain, with around 20%, 50%, and 75% reductions at 10 mg/kg, 30 mg/kg and 100 mg/kg oral doses, respectively. As expected, the peripheral PD effects were greater with almost complete inhibition of Ser935 phosphorylation in all peripheral tissues (lung, spleen, and kidney) at all doses. A single-dose (45 mg/kg) time-course *in vivo* pharmacology experiment for compound **7** in mice was also conducted (Figure 2b). In the study, the maximal reductions of Ser935 phosphorylation were observed at 1 h after oral administration, with around 50% reduction in brain and 80% reduction in both kidney and lung.

Table 4. Developability profile of compound **7**

compound	**7**
Fu% in blood/brain (rat)	3.2/1.0
Fu% in blood/brain (mouse)	3.1/1.0
Fu% in serum (human)	5.9
AMP (nm/s)	480
CYP inhibition pIC_{50} (3A4)	3.8
*h*PXR pEC_{50}	<4.3
OATP1B1 pIC_{50}	4.9
*h*ERG binding pIC_{50}	<4.2

Having demonstrated good *in vivo* pharmacology in rodents, compound **7** was further evaluated for its developability profile (Table 4). The unbound fractions of **7** in blood and brain were determined to be 3.2% and 1.0%, respectively, in rat, in good agreement with the values in mouse (3.1% and 1.0%, respectively). In addition, a good unbound fraction property of **7** was also observed in human serum wherein a 5.9% unbound fraction was observed. The high passive permeability of the compound was also confirmed in the artificial membrane permeability assay (480 nm/s). Compound **7** demonstrated no meaningful inhibition on human CYP3A4 (pIC_{50} = 3.8), OATP1B1 (pIC_{50} < 4.9), and PXR (pIC_{50} < 4.3), suggesting low concern for drug-drug interactions. Further, the *h*ERG binding assay was conducted to evaluate the preliminary cardiac safety, and the compound was determined to have a low risk of QT interval prolongation (*h*ERG pIC_{50} < 4.2).

The synthesis of compound **7** was shown in Scheme 1. Treatment of 2,4-dichloro-7H-pyrrolo-[2,3-d]pyrimidine with sodium ethoxide in ethanol gave intermediate **23**, which then reacted with 4-methylbenzene-1-sulfonyl chloride in the presence of sodium hydride in DMF under room temperature to afford compound **24**. Amide coupling reaction between 3-methoxy-4-nitrobenzoic acid and morphine proceeded smoothly in the presence of EDC and HOBT to provide intermediate **7a**, which was subjected to the hydrogenation reaction to give aniline intermediate **7b**. The final product **7** was obtained through Buchwald coupling reaction between **24** and **7b** using $Pd_2(dba)_3$ as the catalyst and Xphos as the ligand.

In summary, we discovered a series of 7*H*-pyrrolo[2,3-*d*]pyrimidin-2-amine derivatives as potent LRRK2 kinase inhibitors through kinase-focused set screening (KCS). Further optimization of the kinase selectivity and physicochemical properties led to the discovery of compound **7** with high *in vitro* inhibition of LRRK2 kinase activity and good selectivity over hundreds of other kinases. The compound proved to be CNS penetrant, and *in vivo* pharmacology experiments revealed significant inhibition of Ser935 phosphorylation of LRRK2 in brain of both rats (30 mg/kg and 100 mg/kg) and mice (45 mg/kg) following oral administration. In addition, compound **7** demonstrated good developability profile which enabled it to be a good tool for the exploration of LRRK2 biology both *in vitro* and *in vivo*. Further optimization of this series towards a clinical candidate will be reported in due course.

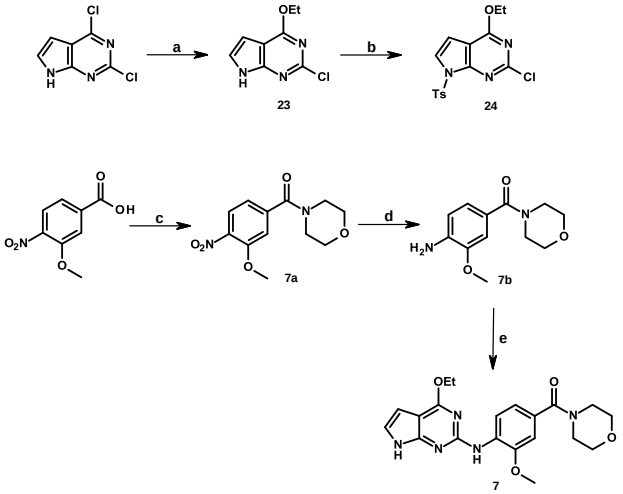

Scheme 1. Synthesis of compound **7**. Reagents and condition: (a) EtONa, EtOH, 90 °C, overnight; (b) TsCl, NaH, DMF, 23 °C, 1 h; (c) morphine, EDC, HOBT, Et_3N, DCM, 23 °C, overnight; (d) Pd/C, H_2, MeOH, 23 °C, overnight; (e) **24**, $Pd_2(dba)_3$, Xphos, K_2CO_3, 2-butanol, 125 °C, overnight.

Acknowledgements

We thank Mr. Liang Huang for HRMS analysis, and Mr. Lijun Ge, Mr. Yan Chen, and Mr. Yong Zhang for their *in vivo* works for compound testing.

Supplementary Material

Supplementary data associated with this article can be found in the online version.

References and Notes

1. Kalia, L. V.; Lang, A. E. *Lancet* **2015**, *386*, 896.
2. *Statistics on Parkinson's*; Parkinson's disease Foundation: New York, 2016; *www.pdf.org/en/parkinson_statistics.*
3. Kalia, L. V.; Kalia, S. K.; Lang, A. E. *Mov. Disord.* **2015**, *30*, 1442.
4. Kalinderi, K.; Bostantjopoulou, S.; Fidani, L. *Acta. Neurol. Scand.* **2016**, *134*, 314.
5. Lee, B. D.; Dawson, V. L.; Dawson, T. M. *Trends Pharmacol. Sci.* **2012**, *33*, 365.
6. Cookson, M. R. *Nat. Rev. Neurosci.* **2010**, *11*, 791.
7. Galatsis, P.*Expert. Opin. Ther. Pat.* **2017**, *27*, 667.
8. Christensen, K. V.; Smith, G. P.; Williamson, D. S. *Prog. Med. Chem.* **2017**, *56*, 37.
9. Estrada, A. A.; Chan, B. K.; Baker-Glenn, C.; Beresford, A.; Burdick, D. J.; Chambers, M.; Chen, H.; Dominguez, S. L.; Dotson, J.; Drummond, J.; Flagella, M.; Fuji, R.; Gill, A.; Halladay, J.; Harris, S. F.; Heffron, T. P.; Kleinheinz, T.; Lee, D. W.; Le Pichon, C. E.; Liu, X.; Lyssikatos, J. P.; Medhurst, A. D.; Moffat, J. G.; Nash, K.; Scearce-Levie, K.; Sheng, Z.; Shore, D. G.; Wong, S.; Zhang, S.; Zhang, X.; Zhu, H.; Sweeney, Z. K. *J. Med. Chem.* **2014**, *57*, 921.
10. Scott, J. D.; DeMong, D. E.; Greshock, T. J.; Basu, K.; Dai, X.; Harris, J.; Hruza, A.; Li, S. W.; Lin, S. I.; Liu, H.; Macala, M. K.; Hu, Z.; Mei, H.; Zhang, H.; Walsh, P.; Poirier, M.; Shi, Z. C.; Xiao, L.; Agnihotri, G.; Baptista, M. A.; Columbus, J.; Fell, M. J.; Hyde, L. A.; Kuvelkar, R.; Lin, Y.; Mirescu, C.; Morrow, J. A.; Yin, Z.; Zhang, X.; Zhou, X.; Chang, R. K.; Embrey, M. W.; Sanders, J. M.; Tiscia, H. E.; Drolet, R. E.; Kern, J. T.; Sur, S. M.; Renger, J. J.; Bilodeau, M. T.; Kennedy, M. E.; Parker, E. M.; Stamford, A. W.; Nargund, R.; McCauley, J. A.; Miller, M. W. *J. Med. Chem.* **2017**, *60*, 2983.
11. Henderson, J. L.; Kormos, B. L.; Hayward, M. M.; Coffman, K. J.; Jasti, J.; Kurumbail, R. G.; Wager, T. T.; Verhoest, P. R.; Noell, G. S.; Chen, Y.; Needle, E.; Berger, Z.; Steyn, S. J.; Houle, C.; Hirst, W. D.; Galatsis, P. *J. Med. Chem.* **2015**, *58*, 419.
12. Troxler, T.; Greenidge, P.; Zimmermann, K.; Desrayaud, S.; Druckes, P.; Schweizer, T.; Stauffer, D.; Rovelli, G.; Shimshek, D. R. *Bioorg. Med. Chem. Lett.* **2013**, *23*, 4085.
13. Garofalo, A. W.; Adler, M.; Aubele, D. L.; Brigham, E. F.; Chian, D.; Franzini, M.; Goldbach, E.; Kwong, G. T.; Motter, R.; Probst, G. D.; Quinn, K. P.; Ruslim, L.; Sham, H. L.; Tam, D.; Tanaka, P.; Truong, A. P.; Ye, X. M.; Ren, Z. *Bioorg. Med. Chem. Lett.* **2013**, *23*, 1974.
14. Nichols, P. L. E.; Andrew J.; Bamborough, P.; Jandu, K. S.; Philps, O. J.; Andreotti, D. WO2011038572. **2011**.
15. Ding, X.; Liu, Q.; Long, K.; Sang, Y.; Stasi, L. P.; Wan, Z.; Xu, Q.; Edge, C. WO2015113451A1. **2015**.
16. Ding, X.; Long, K.; Sang, Y.; Stasi, L. P.; Wan, Z.; Zhao, B.; Edge, C. WO2015113452A1. **2015**.
17. Reith, A. D.; Bamborough, P.; Jandu, K.; Andreotti, D.; Mensah, L.; Dossang, P.; Choi, H. G.; Deng, X.; Zhang, J.; Alessi, D. R.; Gray, N. S. *Bioorg. Med. Chem. Lett.* **2012**, *22*, 5625.
18. Ding, X.; Dai, X.; Long, K.; Peng, C.; Andreotti, D.; Bamborough, P.; Eatherton, A. J.; Edge, C.; Jandu, K. S.; Nichols, P. L.; Philps, O. J.; Stasi, L. P.; Wan, Z.; Xiang, J. N.; Dong, K.; Dossang, P.; Ho, M. H.; Li, Y.; Mensah, L.; Guan, X.; Reith, A. D.; Ren, F. *Bioorg. Med. Chem. Lett.* **2017**, *27*, 4034.
19. Steger, M.; Tonelli, F.; Ito, G.; Davies, P.; Trost, M.; Vetter, M.; Wachter, S.; Lorentzen, E.; Duddy, G.; Wilson, S.; Baptista, M. A.; Fiske, B. K.; Fell, M. J.; Morrow, J. A.; Reith, A. D.; Alessi, D. R.; Mann, M. elife **2016**, *5*.
20. Ito, G.; Katsemonova, K.; Tonelli, F.; Lis, P.; Baptista, M. A.; Shpiro, N.; Duddy, G.; Wilson, S.; Ho, P. W.; Ho, S. L.; Reith, A. D.; Alessi, D. R. *Biochem. J.* **2016**, *473*, 2671.
21. Ancliff, R. A.; Atkinson, F. L.; Barker, M. D.; Box, P. C.; Daniel, C.; Gore, P. M.; Guntrip, S. B.; Hasegawa, M.; Inglis, G. G. A.; Kano, K.; Miyazaki, Y.; Patel, V. K.; Ritchie, T. J.; Swanson, S.; Walker, A. L.; Wellaway, C. R.; Woodrow. WO2007042299. **2007**.
22. J. Salas Solana, J.; Almansa Rosales, C.; Soliva, R.; Fontes Ustrell, M.; Vendrell Escobar, M. WO2008119792. **2008**.
23. Hitchcock, S. A.; Pennington, L. D. *J. Med. Chem.* **2006**, *49*, 7559–7583.
24. Bain, J.; Plater, L.; Elliott, M.; Shpiro, N.; Hastie, C. J.; McLauchlan, H.; Klevernic, I.; Arthur, J. S.; Alessi, D. R.; Cohen, P. *Biochem. J.* **2007**, *408*, 297–315.
25. Chartier, M.; Chenard, T.; Barker, J.; Najmanovich, R. *PeerJ*. **2013**, *1*, e126.
26. Sievers, F.; Wilm, A.; Dineen, D.; Gibson, T. J.; Karplus, K.; Li, W.; Lopez, R.; McWilliam, H.; Remmert, M.; Soding, J.; Thompson, J. D.; Higgins, D. G. *Mol. Syst. Biol.* **2011**, *7*, 539.
27. Hatcher, J. M.; Zhang, J.; Choi, H. G.; Ito, G.; Alessi, D. R.; Gray, N. S. *ACS Med. Chem. Lett.* **2015**, *6*, 584.
28. Chen, H.; Chan, B. K.; Drummond, J.; Estrada, A. A.; Gunzner-Toste, J.; Liu, X.; Liu, Y.; Moffat, J.; Shore, D.; Sweeney, Z. K.; Tran, T.; Wang, S.; Zhao, G.; Zhu, H.; Burdick, D. J. *J. Med. Chem.* **2012**, *55*, 5536–5545.
29. The human biological samples were sourced ethically and their research use was in accord with the terms of the informed consents. All studies were conducted in accordance with the GSK Policy on the Care, Welfare and Treatment of Laboratory Animals and were reviewed the Institutional Animal Care and Use Committee either at GSK or by the ethical review process at the institution where the work was performed.
30. Fabian, M. A.; Biggs, W. H., 3rd; Treiber, D. K.; Atteridge, C. E.; Azimioara, M. D.; Benedetti, M. G.; Carter, T. A.; Ciceri, P.; Edeen, P. T.; Floyd, M.; Ford, J. M.; Galvin, M.; Gerlach, J. L.; Grotzfeld, R. M.; Herrgard, S.; Insko, D. E.; Insko, M. A.; Lai, A. G.; Lelias, J. M.; Mehta, S. A.; Milanov, Z. V.; Velasco, A. M.; Wodicka, L. M.; Patel, H. K.; Zarrinkar, P. P.; Lockhart, D. J. *Nat. Biotechnol.* **2005**, *23*, 329.
31. Young, R. J.; Green, D. V.; Luscombe, C. N.; Hill, A. P. *Drug Discov. Today* **2011**, *16*, 822.

32. Dzamko, M.; Deak, M.; Hentati, F.; Reith, A.D.; Prescott, A.R.; Alessi, D.R.; Nichols, R.J. *Biochem. J.* **2010**, *430*, 405.